Direction Finding and Ray Tracing of Medium-Frequency Burst Auroral Radio Emissions

T. M. Godfrey, J. LaBelle

Dartmouth College, Department of Physics and Astronomy

Introduction

This study investigates medium-frequency burst (MFB) auroral radio emissions using a combination of direction-of-arrival (DOA) measurements and coincident incoherent scatter radar (ISR) electron density observations. Building on prior studies that examined MFB using either DOA or ISR measurements, this work brings these complementary diagnostics together for a case study event. MFB typically spans 1.5–4.5 MHz, is thought to originate in the ionospheric topside, and often appears just before or after auroral substorm onset (Weatherwax et al., 1994). Ray tracing simulations are used to evaluate the proposed MFB generation mechanism.

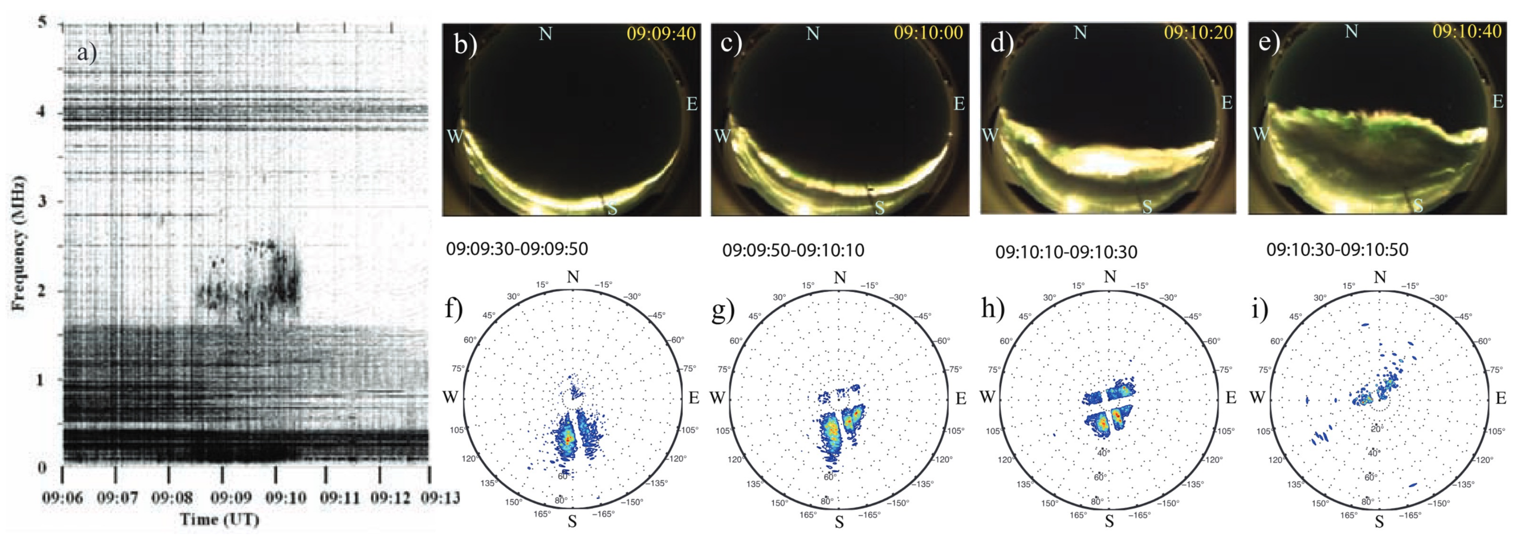

Figure 1: MFB study from November 20, 2007 by Bunch [2009] at Toolik Lake, AK. (a) Spectrogram of the MFB event observed with ground-based interferometer. (b-e) Optical data detailing auroral arcs moving Northward. (f-i) Distributions of DOA of the MFB. This study did not include coincident ISR electron density data.

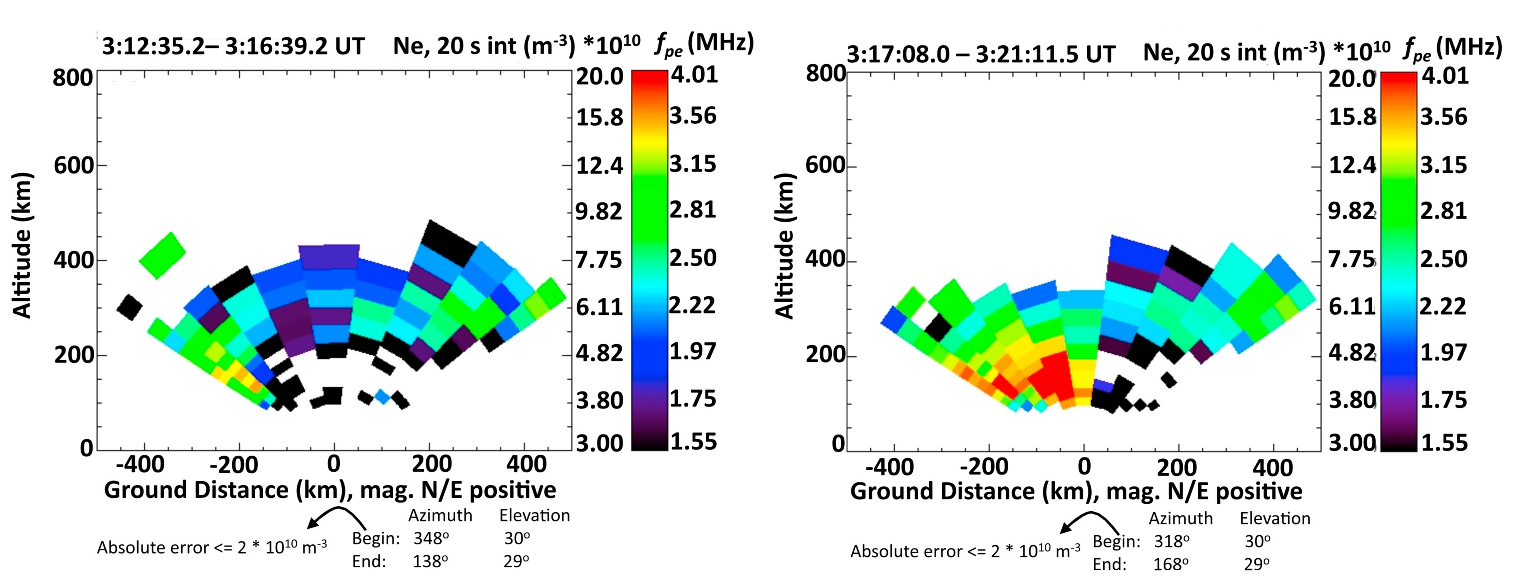

Figure 2: Sondrestrom ISR electron density data from a full composite scan data just before (left) and after (right) the onset of MFB from March 25, 2006 by Broughton [2012]. This study did not include coincident DOA data from ground-based interferometer observations.

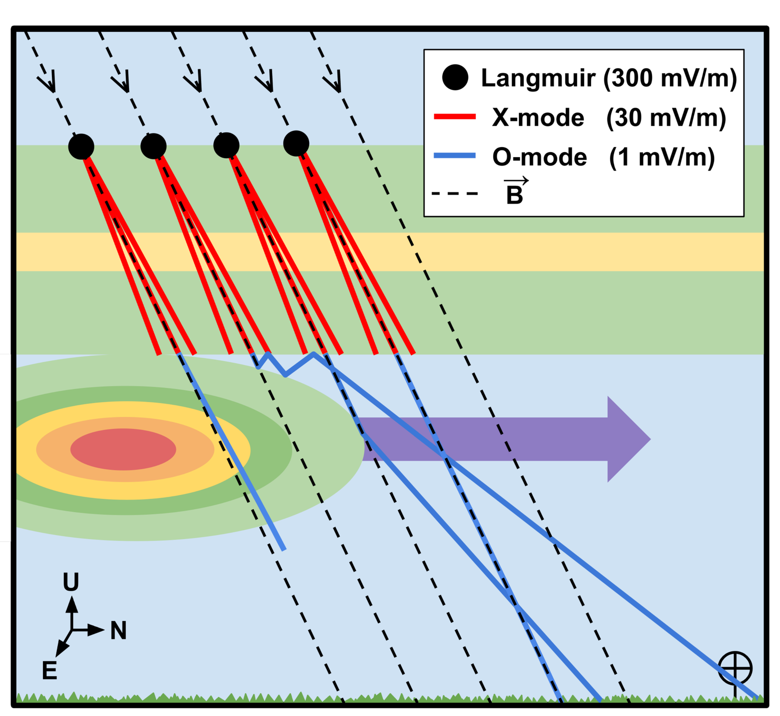

Figure 3: Schematic illustrating how MFB is formed and observed based on LaBelle [1997, 2011]. Electrostatic waves convert to electromagnetic waves at the plasma frequency. Upon reaching the lower plasma frequency cutoff, RX-mode converts to LO-mode only when parallel to the magnetic field.

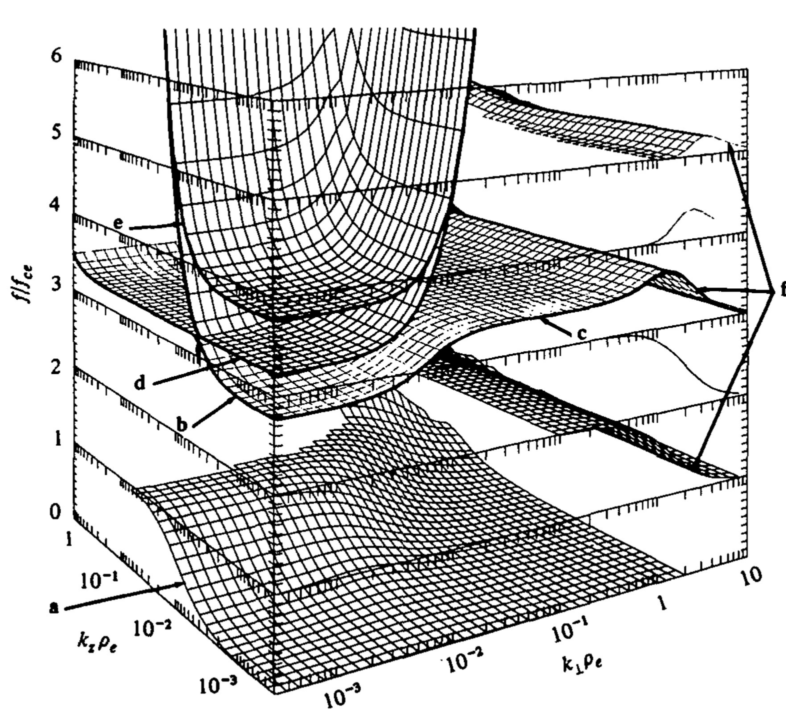

Figure 4: Dispersion surfaces of plasma waves in frequency versus wave vector components by André [1985]. Various wave modes are shown: (a-f) Whistler, RX, upper hybrid, plasma frequency, X, electron Bernstein harmonics.

References

1. André, M. (1985). Dispersion surfaces. *Journal of Plasma Physics, 33*(1), 1–19. doi: 10.1017/S0022377800002270
2. Bonnell, J. W., Ludlam, M., Slagle, A., Goodrich, K., & LaBelle, J. W. (2025). The Electric Field Instrument (EFI) for the TRACERS Mission. *Space Science Reviews, 221*(6), 80.
3. Broughton, M. C., LaBelle, J., Roberg-Clark, G. T., McCready, M., & Bunch, N. L. (2012). Experimental tests of a topside generation mechanism for auroral medium frequency radio emissions. *Journal of Geophysical Research: Space Physics, 117*(A12), A12309. doi: 10.1029/2012JA018034
4. Bunch, N. L., LaBelle, J., Weatherwax, A. T., Hughes, J. M., & Lummerzheim, D. (2009). Experimental tests of the generation mechanism of auroral medium frequency burst radio emissions. *Journal of Geophysical Research: Space Physics, 114*(A9), A09302. doi: 10.1029/2008JA013993
5. Cervera, M. A. (2016). *PHaRLAP: Provision of High-frequency Raytracing Laboratory for Propagation studies* [Computer software]. Defence Science and Technology Group.
6. Halekas, J. S., Hansen, C., Ruhunusiri, S., Sheets, D., Washington, A., Beals, R. M., ... & Miles, D. M. (2025). The TRACERS analyzer for cusp electrons. *Space science reviews, 221*(1), 21.
7. Kletzing, C. A., Mozer, F. S., & Torbert, R. B. (1998). Electron temperature and density at high latitude. *Journal of Geophysical Research: Space Physics, 103*(A7), 14837–14845. doi: 10.1029/98JA00962
8. LaBelle, J., Shepherd, S. G., & Trimpi, M. L. (1997). Observations of auroral medium frequency bursts. *Journal of Geophysical Research: Space Physics, 102*(A10), 22221–22231. doi: 10.1029/97JA01905
9. LaBelle, J. (2011). An explanation for the fine structure of MF burst emissions. *Geophysical Research Letters, 38*, L03105. doi: 10.1029/2010GL046218
10. Weatherwax, A. T., LaBelle, J., & Trimpi, M. L. (1994). A new type of auroral radio emission observed at medium frequencies (~1350–3700 kHz) using ground-based receivers. *Geophysical Research Letters, 21*(24), 2753–2756. doi: 10.1029/94GL02512

Methodology

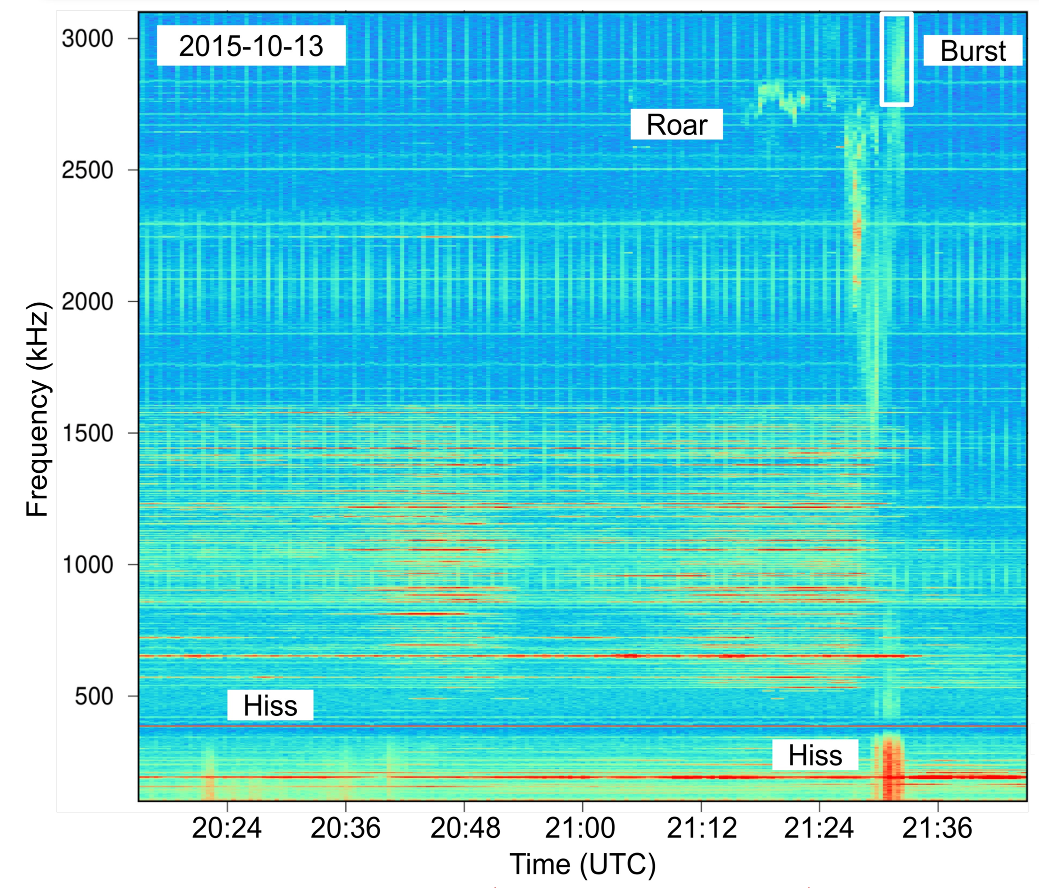

Figure 5: Spectrogram of case study MFB event (white box) over the course of about an hour to give more context for the emission. Two other types of auroral radio emissions: 2nd cyclotron harmonic and hiss can also be seen near the MFB. The fading of the AM radio band seen between 600 and 1750 kHz around 21:30 UTC indicates the onset of an auroral substorm.

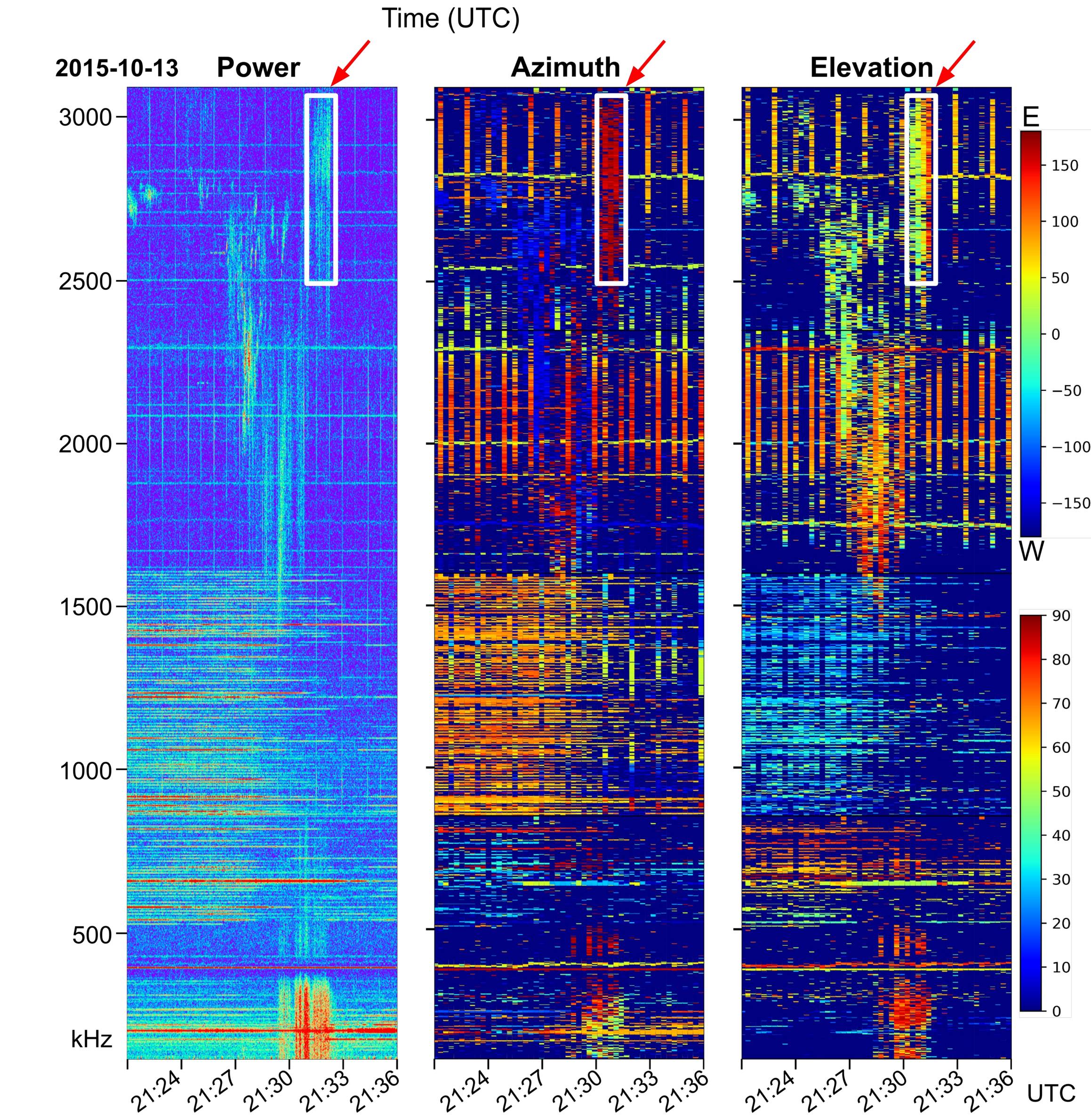

Figure 6: Power (left), azimuth (middle), and elevation (right) spectrograms for the MFB case study event on October 13, 2015. The burst spans 1500–3100 kHz. A box selection tool was developed to analyze these spectrograms, remove interference signals, and filter by power and frequency more efficiently. The white box indicates the region that is analyzed in greater detail (ray tracing study), because Sondrestrom ISR data were available. The vertical interference lines are the ISR radio signature. The signal is notched around 450 kHz to eliminate a strong local beacon signal.

Figure 7: DOA data were collected with a 5-antenna array in Sondrestrom, Greenland (73.3° magnetic latitude). The larger array is used for the higher frequency channels (850–3100 kHz), and the smaller array is used for the lower frequency channel (100-850 kHz). Both arrays share the reference antenna shown.

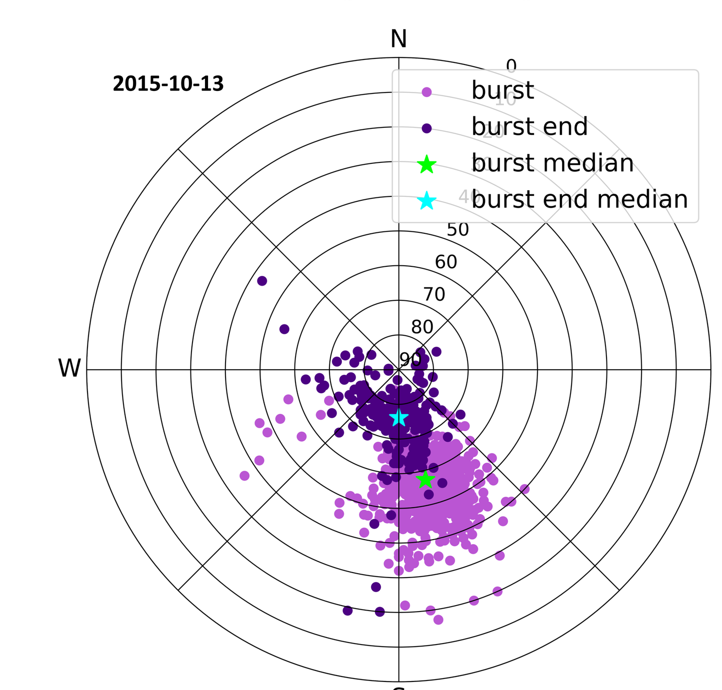

Figure 8: October 13, 2015 MFB event DOA. Azimuth is around and elevation is radial. Light purple is the entire MFB with median azimuth (elevation): 166° (57°). Dark purple is the last half of MFB with median azimuth (elevation): 180° (76°). This indicates poleward movement.

Ray Tracing

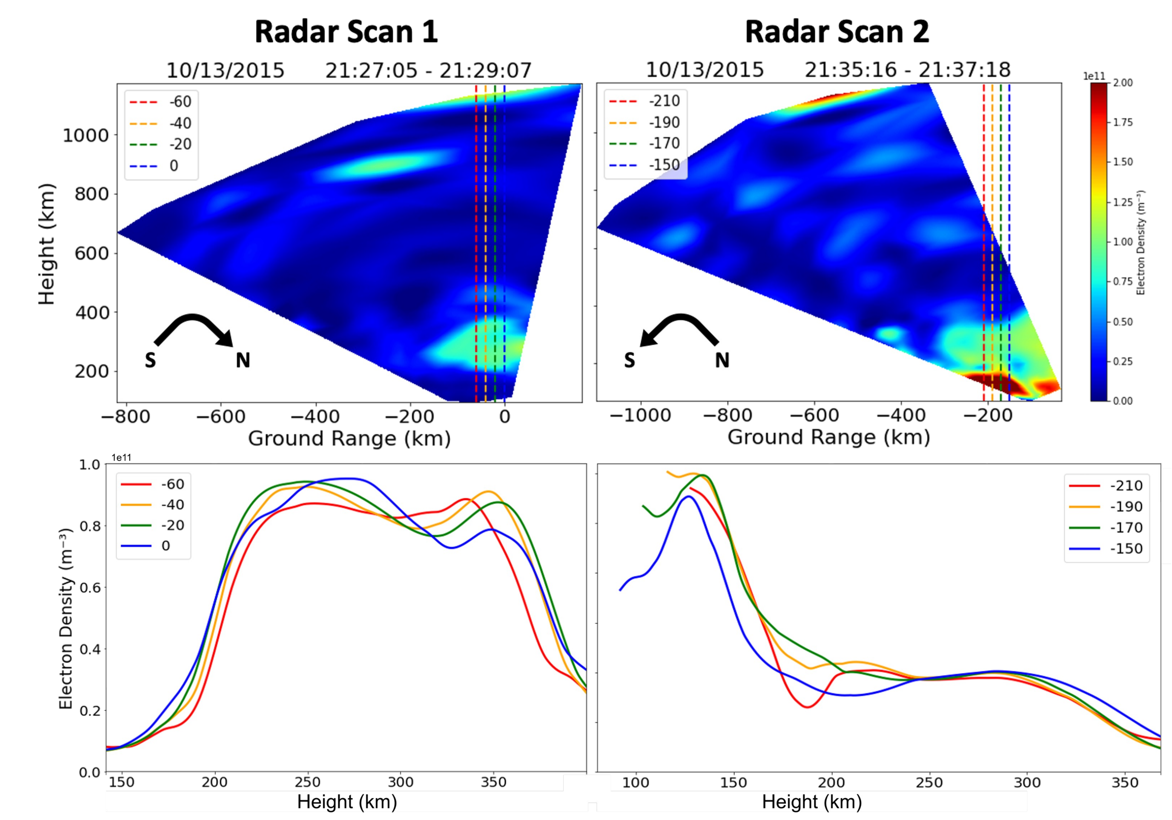

Figure 9: The processing of October 13, 2015 Sondrestrom ISR electron density half-composite scan data. The left column shows the F-region just before the MFB event onset, and the right column shows the E-region enhancement just after the event occurred. This data is available through Madrigal under Sondrestrom ISR. The first row is a cubic spline interpolation on the raw density data, along with four vertical slices in the regions of interest. The second row shows each of those slices of electron density vs. height, with the legend indicating the corresponding ground range. Ground ranges of -20 and -170 (green in both) were chosen to fit the background F-region and enhanced density E-region, respectively.

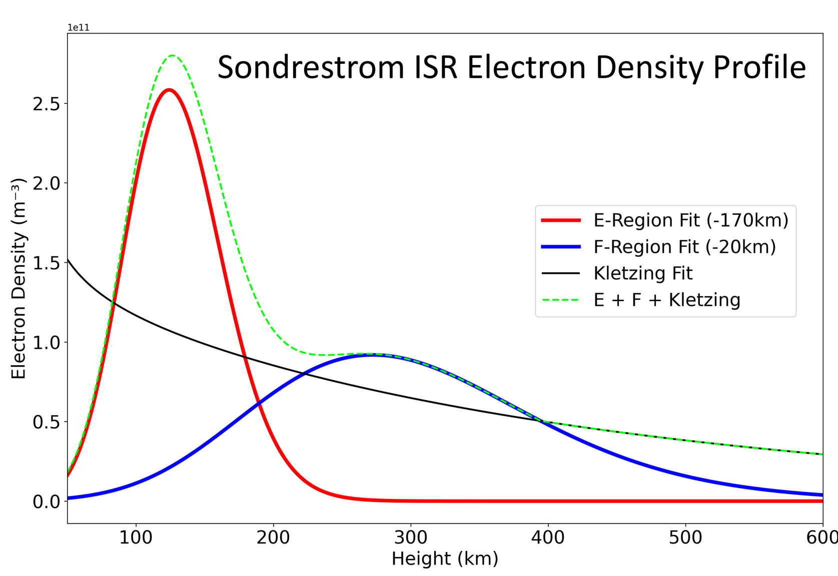

Figure 10: Electron density as a function of height for Chapman profiles fit to the E-region in red and F-region in blue. A function for ionospheric conditions at high latitudes is used for the electron density above 400 km in black following Kletzing and Mozer [1998]. For ray tracing, the linear combination of the two Chapman functions with an E-region max of $2.8\times10^{11}\ m^{-3}$ (green dashed) is used.

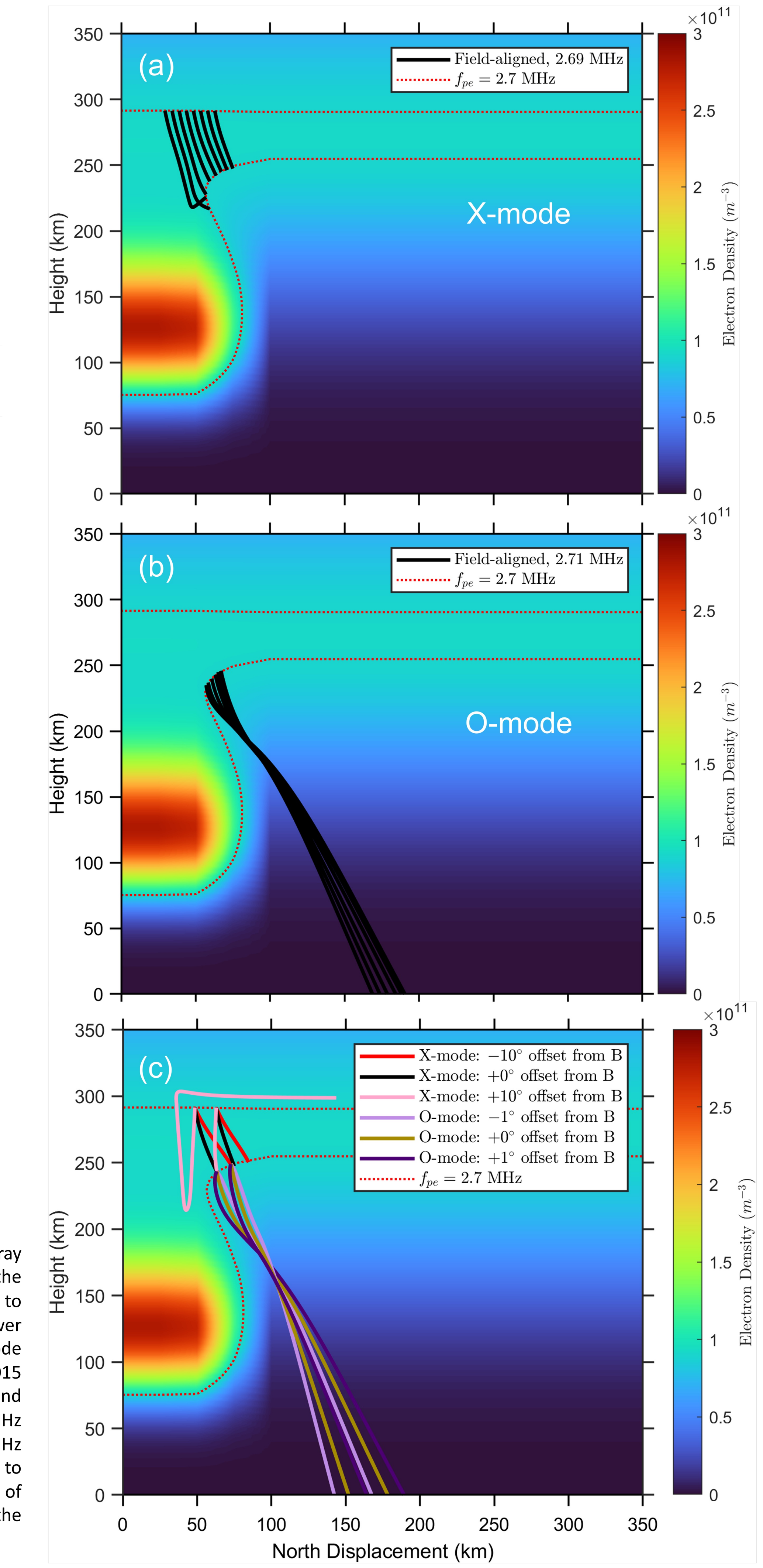

Figure 11: The three figures to the right are MFB ray traces using the open-source PHaRLAP ray tracing program by Cervera [2016]. These ray traces are done in effectively 3D to include the geomagnetic field, by using a thin longitudinal plane. The purpose of the X-mode traces is to evaluate the possibility of rays being parallel to the magnetic field when reaching the lower plasma frequency contour, since only these can convert to O-mode. The purpose of the O-mode traces is to match the final elevation angles with the DOA observations for the October 13, 2015 MFB event. (a) X-mode rays at 2.69 MHz started parallel to the magnetic field at heights and ground ranges along the upper 2.70 MHz plasma frequency line. (b) O-mode rays at 2.71 MHz started parallel to the magnetic field at heights and ground ranges along the lower 2.70 MHz plasma frequency line. (c) Selected X- and O-mode rays starting offset or parallel (0° offset) to the magnetic field at 0.01 MHz below and above the plasma frequency, respectively. Analysis of the magnetic field alignment for the X-mode rays at the cutoff and final elevation angles for the O-mode rays at the ground will be done to evaluate this MFB mechanism.

TRACERS

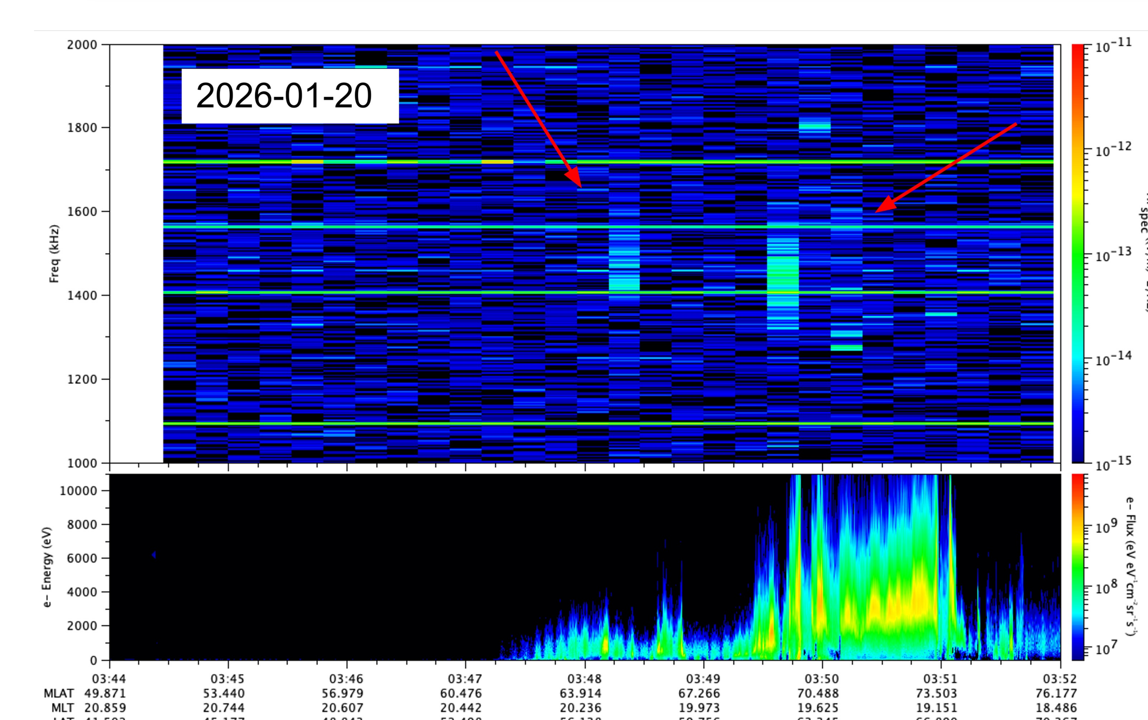

Figure 12: Potential MFB emission spanning 1300–1600 kHz observed by the TRACERS satellite mission. MFB is difficult to observe from satellites due to its short duration. The top panel shows a spectrogram from the onboard electric field instrument led by Bonnell et al. [2025]. The emission coincides with enhanced electron flux in the bottom panel, measured by the onboard analyzer for cusp electrons led by Halekas et al. [2025]. Six potential MFB events have been identified in nightside passes through the auroral zone in two months of 2026 TRACERS data. Future work will apply the ray tracing techniques described above to these events.

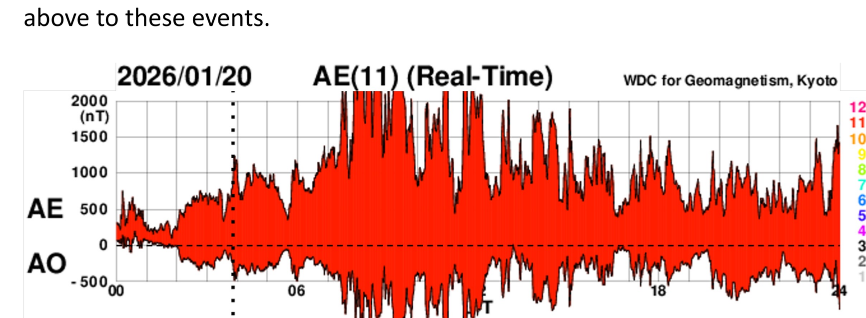

Figure 13: Geophysical index data corresponding to the MFB event observed by TRACERS. The start of the MFB event is given by the vertical black dash. The increase in AE index corresponds to the onset of an auroral substorm, strongly suggesting that this emission could be MFB.

Contact: tedi.m.godfrey.gr@dartmouth.edu

Financial support provided by NSF Grant AGS-1915058 to Dartmouth College and NASA New Hampshire Space Grant 80NSSC20M0051. Some results shown in this poster were obtained using the HF propagation toolbox, PHaRLAP, created by Dr. Manuel Cervera, Defence Science and Technology Group, Australia (manuel.cervera@dsto.defence.gov.au). This toolbox is available by request from its author. Thanks to David McGaw for instrumentation engineering.